Cancer Research

TGFβ-Activated USP27X Deubiquitinase Regulates Cell Migration and Chemoresistance via Stabilization of Snail1

Guillem Lambies[1,2], Martina Miceli[1], Catalina Martínez-Guillamon[1], Rubén Olivera-Salguero[1], Raúl Peña[1], Carolina-Paola Frías[1], Irene Calderón[1], Boyko S. Atanassov[3], Sharon Y. R. Dent[4], Joaquín Arribas[5,6,7], Antonio García de Herreros[1,2], and Víctor M. Díaz[1,2]

Abstract

In cancer cells, epithelial-to-mesenchymal transition (EMT) is controlled by Snail1, a transcriptional factor also required for the activation of cancer-associated fibroblasts (CAF). Snail1 is short-lived in normal epithelial cells as a consequence of its coordinated and continuous ubiquitination by several F-box–specific E3 ligases, but its degradation is prevented in cancer cells and in activated fibroblasts. Here, we performed an siRNA screen and identified USP27X as a deubiquitinase that increases Snail1 stability. Expression of USP27X in breast and pancreatic cancer cell lines and tumors positively correlated with Snail1 expression levels. Accordingly, downregulation of USP27X decreased Snail1 protein in several tumor cell lines. USP27X depletion impaired Snail1-dependent cell migration and invasion and metastasis formation and increased cellular sensitivity to cisplatin. USP27X was upregulated by TGFβ during EMT and was required for TGFβ-induced expression of Snail1 and other mesenchymal markers in epithelial cells and CAF. In agreement with this, depletion of USP27X prevented TGFβ-induced EMT and fibroblast activation. Collectively, these results indicate that USP27X is an essential protein controlling Snail1 expression and function and may serve as a target for inhibition of Snail1-dependent tumoral invasion and chemoresistance.

Significance: These findings show that inhibition of USP27X destabilizes Snail1 to impair EMT and renders tumor cells sensitive to chemotherapy, thus opening new strategies for the inhibition of Snail1 expression and its protumoral actions.

Graphical Abstract: http://cancerres.aacrjournals.org/content/canres/79/1/33/F1.large.jpg.

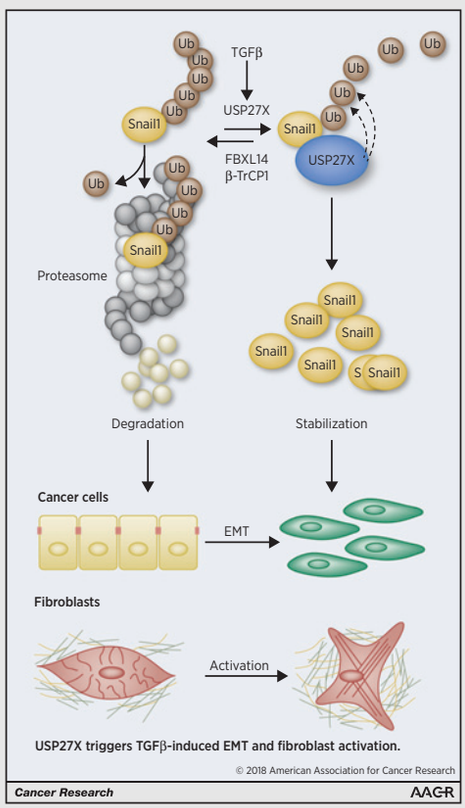

[1]Programa de Recerca en Càncer, Institut Hospital del Mar d'Investigacions Mèdiques (IMIM), Unidad Asociada CSIC, Barcelona, Spain. [2]Departament de Ciències Experimentals i de la Salut, Universitat Pompeu Fabra (UPF), Barcelona, Spain. [3]Department of Pharmacology and Therapeutics, Roswell Park Comprehensive Cancer Center, Buffalo, New York. [4]Department of Epigenetics and Molecular Carcinogenesis, Center for Cancer Epigenetics, The University of Texas MD Anderson Cancer Center, Smithville, Texas. [5]Preclinical Research Program, Vall d'Hebron Institute of Oncology (VHIO) CIBERONC, Barcelona, Spain. [6]Institució Catalana de Recerca i Estudis Avançats (ICREA), Barcelona, Spain. [7]Department of Biochemistry and Molecular Biology, Universitat Autònoma de Barcelona, Campus de la UAB, Bellaterra, Spain.

Note: Supplementary data for this article are available at Cancer Research Online (http://cancerres.aacrjournals.org/).

Corresponding Authors: Víctor M. Díaz, Universitat Pompeu Fabra, Doctor Aiguader 88, E-08003, Barcelona, Spain. Phone: 34933160431; E-mail: victor.diaz@upf.edu; and Antonio García de Herreros, agarcia@imim.es

doi: 10.1158/0008-5472.CAN-18-0753

Introduction

The epithelial-to-mesenchymal transition (EMT) is a reversible and highly conserved biological process originally described during embryonic development that shifts epithelial cells toward a mesenchymal phenotype (1). EMT is observed at the invasive tumor front and correlates with enhanced invasiveness and poor clinical prognosis (2). Phenotypically, tumor cells that have undergone an EMT become spindle-shaped and motile and acquire new biological characteristics, such as a higher resistance to chemotherapy (3, 4).

EMT is defined by the downregulation of the epithelial junctional protein E-cadherin, which is preceded by the expression of Snail1 repressor that directly binds to the E-cadherin gene (*CDH1*) promoter inhibiting its transcription (3). Snail1 also plays an active role in the activation of mesenchymal genes, such as Fibronectin (3). Moreover, Snail1 expression enhances resistance to apoptosis and the survival of tumor cells in conditions of stress (3). For all these reasons, Snail1 is considered a key protein controlling EMT.

In accordance with its functions, Snail1 expression in human tumors is associated with tumor progression, enhanced invasiveness, and poor clinical prognosis (1). In pancreatic cancer, carcinoma cells utilize an EMT program for metastatic dissemination (5). In breast tumors, expression of Snail1 and other mesenchymal markers associates with poor clinical parameters and to the particularly aggressive triple-negative breast cancer (TNBC) subtype with a high rate of recurrence and distant metastasis (6). This suggests that Snail1 is a possible target for therapeutic intervention.

Snail1 is a very unstable protein, tightly regulated by ubiquitination by several E3-ubiquitin ligases that catalyze the transfer of ubiquitin (Ub) from the E2-conjugating enzyme to a lysine residue in the substrate protein and the posterior elongation of the Ub chains (7). Snail1 is targeted to the proteasome by several Skp-Culin-Fbox (SCF) E3 ligases (SCF-Fbxw1, SCF-Fbxl14, SCF-Fbxl5, SCF-FbxO11, and SCF-FbxO45) that limit Snail1 expression in epithelial cells (8, 9). Different reports have demonstrated the stabilization of Snail1 with the concomitant downregulation of Snail1 E3 ligases in response to hypoxia, several proapoptotic insults such as γ-irradiation or antineoplastic drugs (10–14).

Ubiquitination is a reversible process, and the action of E3 ligases is antagonized by deubiquitinating enzymes (DUB) that recognize and remove Ub molecules (15). The 98 DUBs described so far are classified as cysteine proteases (Ub-specific proteases (USP), Ub carboxy-terminal hydrolases, ovarian tumor-like proteases (OTU) or "Machado-Joseph disease" proteases (MJD) and zinc metalloenzymes (the JAMM/MPN class). The role of DUBs in cancer is stressed by the low stability exhibited by many oncoproteins and the deregulation of their DUBs observed in tumors (16).

Despite the high number of E3 described targeting Snail1, only one DUB, DUB3 (USP17L2), has been recently shown to deubiquitinate Snail1 (17, 18). In an effort to identify new DUBs acting on Snail1, we have performed an siRNA screening on Snail1 expression in the MDA-MB-231 mammary cancer cell line and identified USP27X as a DUB for Snail1.

Materials and Methods

Cell culture, reagents, and antibodies

Authenticated cell lines were obtained from the European Collection of Authenticated Cell Cultures (ECACC) or the ATCC and supplied by the Cancer Cell Line Repository from IMIM. All cell lines were used for no more than 20 passages and routinely tested for *Mycoplasma* contamination by PCR (19). The generation of murine embryonic fibroblasts (MEF) and cancer-associated fibroblasts (CAF) from MMTV-PyMT tumors has been previously reported (20). Cells were maintained in DMEM (GIBCO-BRL) with 10% heat-inactivated FBS (GIBCO-BRL) at 37°C in 5% CO_2. Where indicated, cells were treated with 5 ng/mL of TGFβ1 (PeproTech), 10 to 100 μmol/L of cisplatin (Calbiochem), 20 μmol/L of the DUB inhibitor PR619 (LifeSensors), 20 μg/mL of cycloheximide (Sigma-Aldrich), or 1 μg/mL of doxycycline (Sigma-Aldrich). The antibodies used in this work were mouse monoclonal antibodies against Snail1 (21) and Myc (clone 9E10; a gift from Dr. Gabriel Gil, IMIM, Barcelona); rabbit anti-fibronectin (Dako); goat anti-lamin B (C-20), goat anti-Snail2 (Slug; both from Santa Cruz); rat anti-HA tag (Roche); rabbit anti-HA tag, rabbit anti-flag, rabbit anti-Myc, mouse anti-tubulin (all from Sigma-Aldrich); rabbit anti-GFP, rabbit anti-H3 (Abcam); goat anti-GST (GE Healthcare); rabbit anti-pSmad2, rabbit anti-Snail1 (Cell Signaling) and rabbit anti-USP27X (human and murine; ref. 22).

DNA constructs for lentiviral and retroviral production and infection

pLex-Snail-F-Luc-Puro (lentiviral) and pMSCV-pLuc-Hygro (retroviral) constructs were kindly provided by Dr. Kang lab and were previously described (23) and used to generate viral stocks. For the doxycycline inducible experiments, we used the lentiviral pF-CMV-TetR-PGK-Hygro; pF-CMV-USP27X-Puro-3xFLAG and pF-CMV-USP27XC/A-Puro-3XFLAG vectors, a gift from Dr. A. Weber (24). For *in vivo* imaging studies, we used the retroviral pLHCX-LUC plasmid, a gift from Dr. C. Fillat. Retroviral pBABE-Snail1-HA was previously described (12). Retroviral pBABE-Puro-hUSP27X-C-V5-FL-WT was obtained after BamHI/SalI subcloning from the corresponding pBABE-Zeo vector (22). In general, lentivirus and retroviruses were produced by transient transfection of HEK293T or 293T Phoenix gag-pol cells, respectively, as previously described (12, 13) and in Supplementary Materials and Methods. To generate MDA-MB-231–expressing Snail-F-Luc and R-Luc, cells were first transduced with the lentivirus for Snail1-F-Luc and selected with puromycin (1 μg/mL) and subsequently infected with the Renilla-Luciferase (R-Luc) retrovirus and selected with hygromycin B (200 μg/mL). To generate MDA-MB-231 expressing USP27X induced by doxycycline, cells were first infected with the TetR lentivirus, selected with hygromycin B, and subsequently transduced with the lentiviral expression system following selection with puromycin, as previously described (24). For the Snail1 rescue experiments, MDA-MB-231 USP27X KO cells were infected with the Snail1-HA retrovirus as described previously (12).

siRNA screening

The siRNA screening was performed according to the manufacturer's instructions (Dharmacon). Specific experimental conditions may be found in Supplementary Materials and Methods.

RNA interference

For stable *USP27X* and *CEZ2* gene silencing, the next MISSION shRNA plasmids (Sigma-Aldrich) were used to produce lentiviral particles: *USP27X* (#1: TRCN0000336909; #2: TRCN0000336851; #3: TRCN0000336912); *OTUD7A*/

CEZANNE2 (#1: TRCN0000425854; #2: TRCN0000050160; #3: TRCN0000423073). After transduction, stable cell lines expressing the shRNA were isolated by puromycin (2.5 μg/mL) selection. For DUBs or Snail1 depletion, cells were transfected using DharmaFECT I (Dharmacon) with the specific synthetic siRNAs for: *SNAI1*; *USP27X* (human and murine); *OTUD7A; VCPIP1*; *MPND*; *YOD1*; *USP15*; *TRABID*; *USPL1* (all from Dharmacon) during 48 and 72 hours for RNA and protein analysis, respectively. ON-TARGETplus Nontargeting siRNAs #2 and #3 (Dharmacon) were used as controls.

Mice tumor xenografting and intravenous tail inoculation

For *in vivo* xenografting experiments, 5×10^5 cells were diluted in cold 100 μL 1:1 PBS-Matrigel (growth factor reduced; #354230, Corning), and subcutaneously inoculated in each flank of 6-week-old NOD/SCID mice. After 30 days, mice were euthanized and tumors were photographed and measured. Volumes (V) were determined by using the formula $V = (\text{width})^2 \times \text{length}/2$. Tail-vein injection experiments were performed with 1×10^6 cells/100 μL and immediately analyzed for *in vivo* bioluminescent determination by using the IVIS 50 Imaging System (Xenogen Imaging Technologies) and the Living Image software 2.60.2. Bioluminescent quantification was performed after intraperitoneal inoculation of 100 μL of luciferin (PerkinElmer) solution (25 mg/mL). All experiments with mice were previously approved by the PRBB Committee for Ethical Animal Research (CEEA AGH-16-0034-P2 and AGH-16-0034-P3) following the EU Directive 2010/63/EU.

Generation of knockout cell lines using CRISPR/Cas9

For USP27X knockout (KO) generation, the CRISPR/Cas9 system for human (MDA-MB-231) and murine (NMuMG and MEFs) cells was transfected with the human (sc-407628) and murine (sc-424918) USP27X CRISPR/Cas9 Knockout plasmids (Santa Cruz), respectively, both consisting of a pool of three guide RNA (gRNA) plasmids and codifying for GFP. Transfected cells were selected with the BD Influx Cell Sorter (Becton and Dickinson) and grown as single clones during 2 to 3 weeks. Positive KO clones were identified by Western blot.

Other methods are described in the Supplementary Information.

Results

Identification of USP27X as a putative Snail1 DUB by an siRNA screening

The fusion protein Snail1-*Firefly*-Luciferase (Snail-F-Luc) has been used to identify E3-ligases controlling Snail1 stability (23). Analysis of F-Luc activity (and *Renilla*-Luc, R-Luc, as control) allows a reliable measure of the stability of the Snail-F-Luc fusion protein as demonstrated after treatment with the proteasome inhibitor MG132 or with the protein synthesis inhibitor cycloheximide (CHX; Supplementary Fig. S1A and S1B). The rapid and concomitant regulation of Snail-F-Luc protein and activity by these compounds demonstrate the low stability of Snail1. Interestingly, Snail1-F-Luc levels were sensitive to DUB inhibition by PR619, a cell-permeable and nonselective DUB inhibitor (Supplementary Fig. S1B and S1C; ref. 25). This PR619 effect suggests the participation of one or more DUBs in the control of Snail1 stability.

We generated MDA-MB-231 cells stably expressing Snail-F-Luc and R-Luc and screened MDA-MB-231-Snail1-F-Luc/R-Luc cells with a library of siRNAs targeting all known DUBs (Human ON-TARGET*plus*; Dharmacon). Four different siRNAs were used for each target and F-Luc/R-Luc ratio was determined after 72 hours of transfection. Five different control siRNAs (CTL#1 to #4 and a pool mix) were used as nontargeting controls to define the basal F-Luc/R-Luc reference value (Fig. 1A, red dotted line). A *SNAI1* siRNA was also included to determine the minimal luciferase activity (Fig. 1A, green squares). MG132 was used as a positive control of stabilization (Fig. 1A, yellow dots). In contrast, PR619 strongly decreased F-Luc activity (Fig. 1A, blue crosses). Following the experimental workflow summarized in Supplementary Fig. S1D, two independent rounds of screening were performed to calculate the F-Luc/R-Luc ratio. Inhibition of 17 DUBs caused a 2-fold decrease of the F-Luc/R-Luc ratio, among them, the previously described Snail1 DUB, DUB3 (Fig. 1A). To narrow down the list, we arbitrarily increased the threshold to 2.5 (Fig. 1A, black dotted line); seven DUBs were selected that decreased at least 2.5-fold the F-Luc/R-Luc ratio and further analyzed to discard false positives (Supplementary Fig. S1D). Four DUBs were validated analyzing the effect of the selected DUBs siRNAs on endogenous Snail1 protein: MPND, VCPIP1, USP27X, and OTUD7A/CEZANNE2 (Supplementary Fig. S2A). A quantitative RT-PCR (qRT-PCR) analysis revealed that the efficiency of DUB depletion by the specific siRNAs was higher than 80% and off-side effects on other DUBs were minimal (Supplementary Fig. S2B). *SNAI1* mRNA levels were not affected by *USP27X*, *MPND*, or *VCPIP1* siRNAs; only *OTUD7A/CEZANNE2 (CEZ2)* siRNA decreased it (Supplementary Fig. S2B).

We tested the capability of the selected DUBs to bind Snail1 after cotransfection and immunoprecipitation; only USP27X clearly interacted with Snail1 (Fig. 1B, right). Interestingly, in the presence of MG132, a faint interaction was also observed with Cezanne2 and MPND (Supplementary Fig. S2C). Ectopic Snail1 was stabilized after cotransfection of USP27X or CEZ2 to a much higher extent than by MPND or VCPIP1 (Fig. 1B, left). The interaction between USP27X and Snail1 was also detected with endogenous proteins in MDA-MB-231 cells (Fig. 1C). Transfection of *USP27X* or *CEZ2* siRNAs to these cells downregulated endogenous Snail1 protein (Fig. 1D). A final confirmation was obtained after stable infection of three independent shRNAs against *USP27X* (Fig. 1E) or *CEZ2* (Supplementary Fig. S2D); both of them also decreased the Snail1-downstream target Fibronectin. Therefore, because USP27X consistently interacts with Snail1 and its inhibition decreases Snail1 protein but not mRNA, we chose it as a *bona fide* Snail1 DUB.

We studied the expression of USP27X and Snail1 in a panel of mammary and pancreatic cancer cell lines, two cell systems where Snail1 associates with malignancy (6, 26). In general, both proteins showed a significant correlation in pancreas and breast cancer cells, although some cells exhibit high Snail1 even with low USP27X (Supplementary Fig. S2E). Inhibition of USP27X in the highly expressing pancreatic RWP-1 and PANC-1 cell lines, or in breast BT-474 cells caused a strong decrease in Snail1 (Fig. 1F), reproducing the results obtained in MDA-MB-231 (Fig. 1D and E). Inversely, ectopic expression of USP27X in SKBR3 cells upregulates the levels of Snail1 and the downstream targets Fibronectin and N-Cadherin (Fig. 1G).

USP27X directly binds to Snail1

The *USP27X* gene is predicted to encode for a 49.6 kDa protein (Uniprot: A6NNY8; refs. 24, 27). This USP27X form interacts with Snail1 and increases the levels of ectopic Snail1 as shown in Fig. 1B. However, the recent generation of specific antibodies against USP27X has demonstrated that the most abundant form of this protein presents a molecular weight of 72 kDa (22). This form is originated through translation using

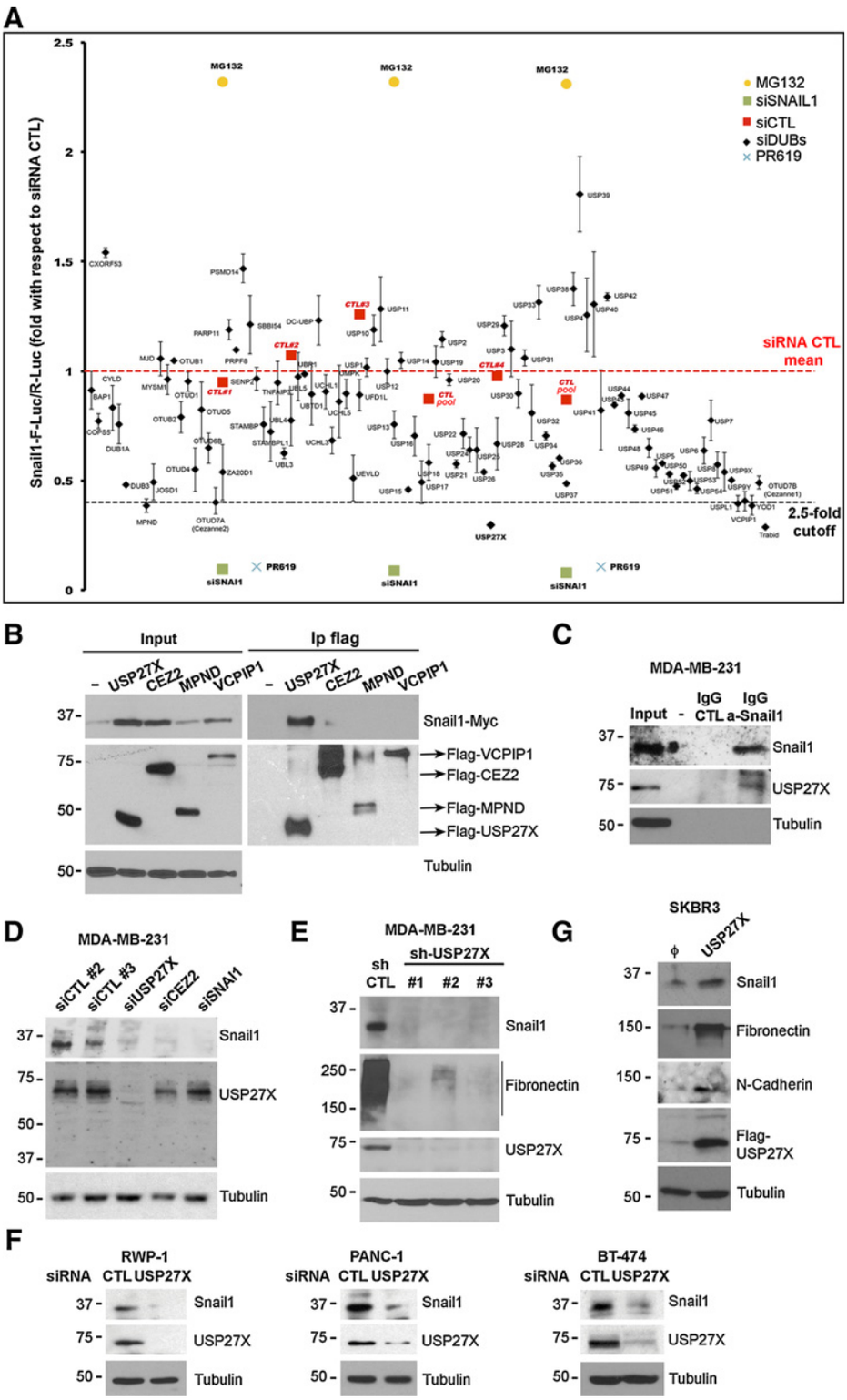

Figure 1.
A DUB siRNA screening identifies USP27X as a putative Snail1 DUB. **A,** Normalized values of Snail1-F-Luc/R-Luc in MDA-MB-231 cells transfected with siRNAs for the indicated DUBs (black diamonds). The basal F-Luc/R-Luc level (siRNA CTL mean) was determined by transfecting individually four control siRNAs (#1 to #4) and a mix of them (CTL pool; red squares). A *SNAI1* siRNA (green squares) was used to define the lower value. Cell treatment with MG132 (yellow dots) or PR619 (blue crosses) was carried out to determine the effect of the inhibition of the proteasomal degradation or the DUB activity. Values represent the mean of two independent screenings and candidates were selected for further analysis when F-Luc/R-Luc ratio decreased more than 2.5-fold (dotted line). **B,** Coimmunoprecipitation of selected Flag-DUBs with ectopic Snail1-Myc analyzed by Western blot. **C**, Endogenous coimmunoprecipitation of Snail1 with USP27X. **D,** MDA-MB-231 cells were transfected with the indicated siRNAs, and Snail1 and USP27X expression was determined by Western blotting. **E,** MDA-MB-231 cells infected with indicated shRNAs (CTL or three different shRNAs for USP27X) were analyzed for Snail1, USP27X, and fibronectin (visualized as a smear band) proteins after being stably selected. **F,** USP27X was depleted by transfecting a specific siRNA in cell lines that show a positive correlation between Snail1 and USP27X (see Supplementary Fig. S2E). **G,** The 72 KDa Flag-USP27X was stably expressed in SKBR3 cells; the expression of Snail1 and EMT markers was analyzed by Western blotting (ϕ, empty vector).

an upstream CTG codon and results in an additional N-terminal extension of 198 amino acids (22). This 72 kDa form was the most abundant detected in MDA-MB-231 cells and was specifically depleted by si*USP27X* and sh*USP27X* (Fig. 1D and E). Overexpression of this 72 KDa form also upregulated Snail1 as shown in Fig. 1G. Pulldown experiments indicate that both the full-length USP27X [FL-USP27X; amino acids (aa) 1-636] and the short form (S-USP27X; aa 198–636) bind to GST-Snail1 (Supplementary Fig. S3A and S3B), suggesting that the N-terminal part of the 72 kDa protein is not required for Snail1 binding and stability. Other data demonstrate that the central region of USP27X (438–561) is involved in the interaction with Snail1 (Supplementary Fig. S3A and S3B).

USP27X–Snail1 association was verified by reverse experiments using recombinant GST-USP27X, which demonstrate that Snail1 and USP27X physically interact and that the binding region is mainly located at the Snail1 C-terminal domain, involving Zn fingers 2 and 3 (Supplementary Fig. S3C and S3D, summarized in S3E). Finally, the direct interaction was also verified using purified recombinant Snail1 and USP27X proteins (Supplementary Fig. S3F). Similar assays were also carried out with Snail2 that did not interact with USP27X.

USP27X shares a high degree of homology with USP22 (82%) and USP51 (70%), and these three proteins constitute a phylogenetically related subfamily (28). Like USP27X, overexpression of USP51, and USP22 to a lower extent upregulated ectopic Snail1 expression (Supplementary Fig. S4A, left). Surprisingly, coimmunoprecipitation experiments indicated that Snail1 interacted with USP27X and USP22 but not with USP51 (Supplementary Fig. S4A, right). Accordingly, GST-Snail1 pulled-down USP22 but not USP51 or any of the other DUBs tested (OTUD7A/CEZANNE2, MPND, VCPIP1; Supplementary Fig. S4B). All these results indicate that USP27X and the close homologue USP22 specifically interact and stabilize Snail1.

USP27X stabilizes and deubiquitinates Snail1

Next, we studied the capability of USP27X to stabilize Snail1 in MDA-MB-231 cells. We used the USP27X form starting from the predicted ATG either wild-type (WT) or an inactive mutant where Cys87, present in the catalytic center, is replaced by an Ala (USP27X C/A; refs. 24, 27). USP27X WT but not the inactive mutant greatly enhanced Snail1 endogenous expression (about 6-fold) without increasing *SNAI1* mRNA (Fig. 2A and B). Snail2 was not significantly modified. Analysis by immunofluorescence revealed that both USP27X and Snail1 colocalized in the nucleus, although USP27X was also observed in the cytoplasm (Fig. 2C). Similar results were obtained transfecting the 72-kDa USP27X long form, which also caused a strong stabilization of ectopic Snail1 in all the subcellular compartments analyzed (cytosol, nucleoplasm, and chromatin; Supplementary Fig. S5A). Inversely, a *USP27X* siRNA caused a strong decrease in Snail1 in its main subcellular localization, the nucleus (Supplementary Fig. S5B and S5C). Curiously, the two forms of endogenous USP27X present a different localization being the short form more abundant in the cytosol, whereas the long form in the nucleus (Supplementary Fig. S5B and S5C). To determine more precisely whether Snail1 is stabilized in the nucleus or the cytosol, we evaluated the action of USP27X on Snail1-SD, a Snail1 mutant highly unstable due to its preferential localization in the cytoplasm and on Snail1-SA or Snail1-LA, mutants that are mainly nuclear (29). As shown in Supplementary Fig. S5D and S5E, the three mutants interacted with USP27X; however, USP27X strongly stabilized Snail1-SD, partially Snail1-LA, and minimally affected Snail1-SA. The lower effect on the nuclear versions of Snail1 suggests that USP27X stabilization is more evident with cytosolic Snail1, which is the one prone to be degraded. However, we cannot rule out the fact that USP27X might target both nuclear and cytosolic Snail1, as suggested by its localization in both compartments.

We also generated MDA-MB-231 cells stably expressing USP27X WT or the C/A mutant under the control of a doxycycline (Doxy) inducible promoter (24). Upon induction of USP27X WT, Snail1 endogenous levels increased gradually until 7-fold; in contrast, the USP27X C/A mutant did not upregulate Snail1 (Fig. 2D). Snail2 expression was only slightly affected by USP27X induction (Supplementary Fig. S6A). Snail1 relative half-life was increased 3-fold by USP27X WT compared with cells transfected with the empty vector or with the USP27X C/A-inactive mutant (Fig. 2E). The lack of Snail1 stabilization with the mutant USP27X is not due to an impaired interaction with Snail1 because both USP27X forms bound similarly (Supplementary Fig. S6B). Ectopic expression of the USP27X increased Snail2 protein stability (Supplementary Fig. S6C) but the effect was much less pronounced than that on Snail1 (Supplementary Fig. S6D).

To determine if Snail1 stabilization is associated with USP27X deubiquitinating activity, we coexpressed Snail1 with ubiquitin and the WT or C/A USP27X forms. After purification of ubiquitinated proteins, Snail1 was detected as a mix of mono- and polyubiquitin forms of high molecular weight (Fig. 2F). Polyubiquitinated Snail1 was strongly decreased upon ectopic expression of WT USP27X (Fig. 2F, left); however, monoubiquitinated Snail1 was relatively resistant to deubiquitination (Fig. 2F). USP27X but not the C/A mutant counteracted the ubiquitination and also the degradation triggered by the β-TrCP1 and FBXL14 ubiquitin ligases (Fig. 2F and G). All these results indicate that USP27X deubiquitinates and stabilizes Snail1.

Because DUB3 has been recently found as a DUB for Snail1/2 (17, 18), we compared this DUB with USP27X. According to our screening data (Fig. 1A), in MDA-MB-231 cells depletion of USP27X was more effective than that of DUB3 in decreasing Snail1 (Supplementary Fig. S6E), whereas USP27X ectopic expression was also more potent in promoting Snail1 stabilization (Supplementary Fig. S6F, compare with Fig. 2E). Both DUBs similarly interacted with Snail1 (Supplementary Fig. S6G).

USP27X depletion decreases proliferation independently on Snail1

We generated MDA-MB-231 cells depleted of USP27X using the CRISPR/Cas9 technology (Fig. 3A). Two independent USP27X knockout (KO) cell clones (named #1 and #2) showed undetectable USP27X (Fig. 3A); in these cells, the levels of Snail1 protein were remarkably downregulated with respect to the control (Fig. 3A) without significant changes in *SNAI1* mRNA (Supplementary Fig. S7A). Other independent clones (KO #3 and KO #4) caused a similar Snail1 protein downregulation (Supplementary Fig. S7B). USP27X KO cells showed a lower growth rate than controls (Fig. 3B), in accordance with the previously reported role of USP27X regulating proliferation (22). The clonogenic capability (Fig. 3C; Supplementary Fig. S7C) was also severely decreased in USP27X KO cells. Elimination of USP27X also retarded the growth of MDA-MB-231 cells when subcutaneously xenografted in NOD/SCID mice (Fig. 3D; Supplementary Fig. S7D). USP27X KO tumors do not express Snail1 and very low levels of fibronectin

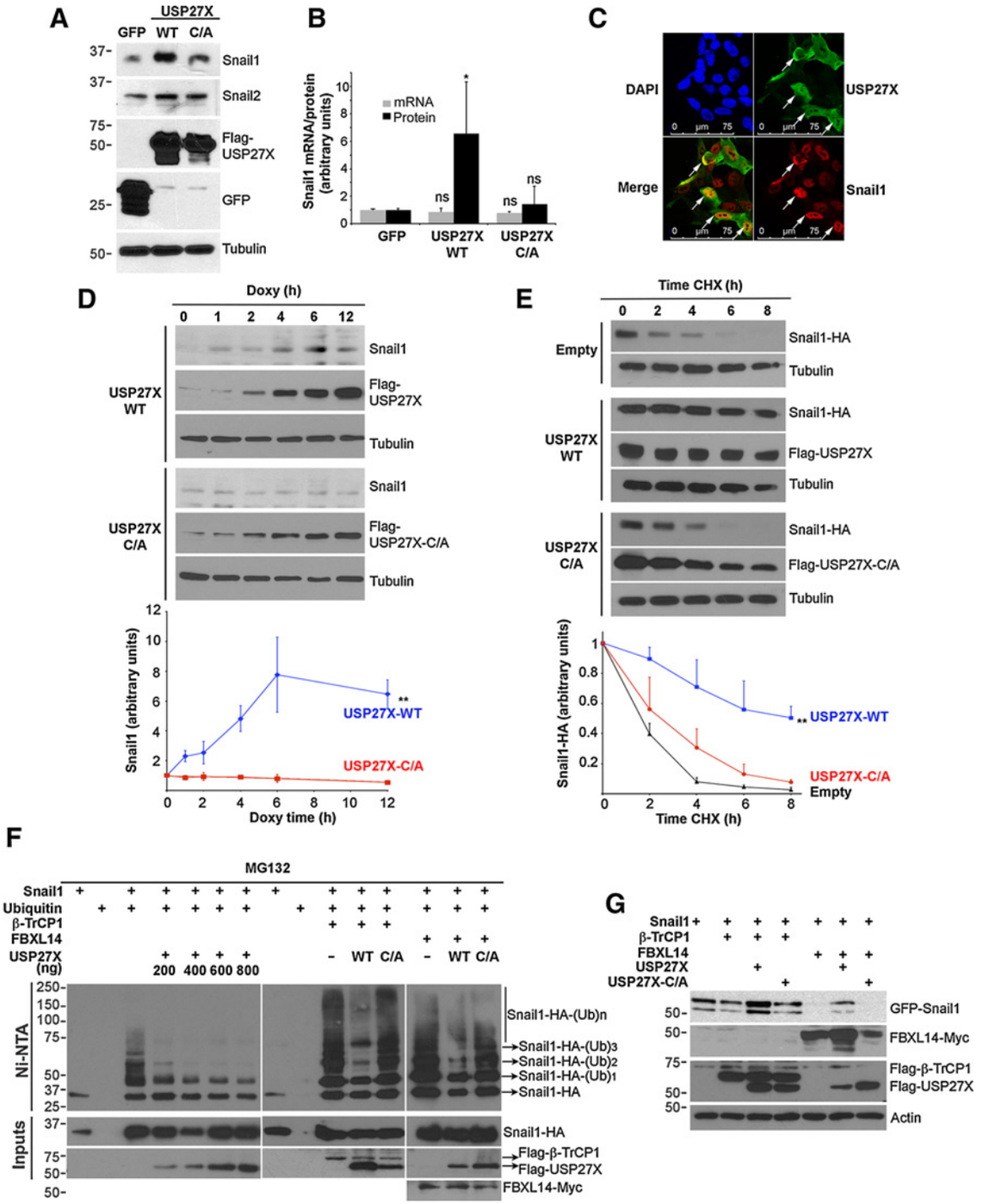

Figure 2.

USP27X expression stabilizes Snail1. **A,** USP27X, either WT or the C/A mutant, were transiently expressed in MDA-MB-231 cells, and endogenous Snail1 and Snail2 levels were determined 48 hours after transfection. **B,** Quantification of endogenous Snail1 protein or mRNA (detected by qRT-PCR) from different transfection experiments ($n = 4$). **C,** Immunofluorescence analysis of Snail1-HA (red) and Flag-USP27X (green) after transient transfection of USP27X in cells stably expressing Snail1-HA. DAPI staining and the merge of Snail1 and USP27X are also shown. Arrows indicate cells expressing USP27X where Snail1 staining is increased. **D,** MDA-MB-231 cells were stably infected with a doxycycline (doxy)-regulated expression plasmid for USP27X (WT or C/A mutant). Endogenous Snail1 expression was monitored at the indicated times after doxy addition. Bottom, densitometric quantification ($n = 3$). **E,** HEK293T cells transiently transfected with Snail1-HA and Flag-USP27X (WT or C/A) were treated with cycloheximide (CHX) for the indicated times and analyzed by Western blotting. Bottom, densitometric quantification ($n = 3$). **F,** The indicated plasmids were transfected together with Ubiquitin-HIS; ubiquitinated proteins were purified by nickel-nitrilotriacetic acid (Ni-NTA) pulldown and Snail1 deubiquitination quantified. The USP27X-mutant C/A was used as a control. **G,** USP27X counteracts Snail1 degradation mediated by the ubiquitinated ligases β-TrCP1 and FBXL14. Data are the mean ± SD, and statistical significance was determined by one-tailed (**B**) or two-tailed (**D** and **E**), unpaired *t* test with *, $P < 0.05$; **, $P < 0.01$; ns, not significant.

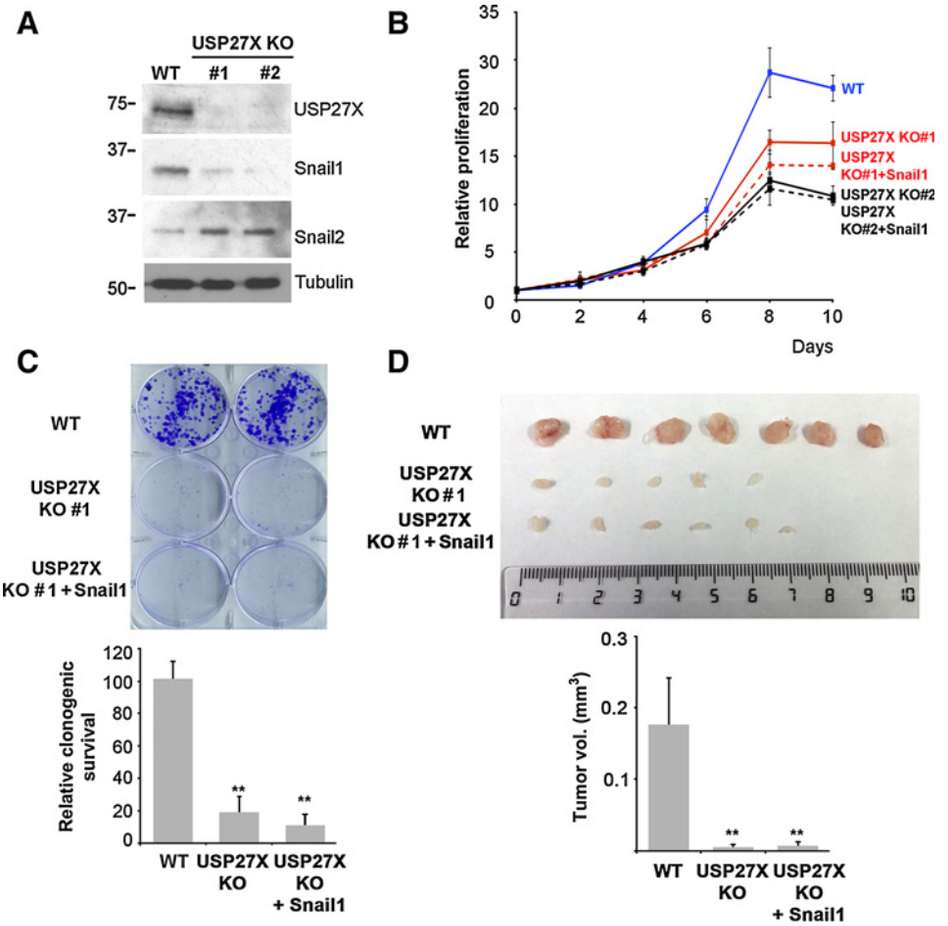

Figure 3.
USP27X depletion retards cell growth. **A,** Western blot analysis of two independent cell lines (#1 and #2) stably selected after CRISPR/Cas9-mediated knockdown of USP27X in MDA-MB-231 cells (*SNAI1* mRNA is shown in Supplementary Fig. S7A). Other CRISPR/Cas9 clones are shown in Supplementary Fig. S7B. **B,** Proliferation of WT (blue line) and USP27 KO cells (#1, red line; #2, black line) and USP27X KO cells infected with a Snail1 retrovirus-expression vector (USP27X KO + Snail1; dotted lines) or with the corresponding CTL virus (USP27X KO). Proliferation was determined by MTT quantification and normalized to time 0 ($n = 3$). **C,** Clonogenic assay carried out with USP27X WT, USP27X KO (#1), or USP27X KO + Snail1 cells (1,000 cells/well; 10 days of cell growth). The picture shows a representative experiment stained with crystal violet. Other experiments with USP27X KO #2 are shown in Supplementary Fig. S7C. The quantification performed with USP27X KO #1 ($n = 3$) was obtained using ImageJ (bottom). **D,** *In vivo* tumor growth of control (WT), USP27X KO, or USP27X KO + Snail1 cells subcutaneously injected in NOD/SCID mice (500,000 cells/flank; 30 days of growth). Data obtained with USP27X KO #2 are shown in Supplementary Fig. S7D. The quantification of the tumors obtained in this experiment is shown at the bottom. Data are the mean ± SD; **, $P < 0.01$.

compared with WT tumors (Supplementary Fig. S7E). Snail1 was infected in USP27X KO cells to obtain levels similar to those detected in control cells (see below); however, Snai1l overexpression did not rescue cell growth (Fig. 3B), colony formation (Fig. 3C), or *in vivo* tumor growth (Fig. 3D), suggesting that USP27X regulates tumor growth by acting on other substrates distinct of Snail1.

USP27X knockdown impairs Snail1-dependent cell invasion, metastasis formation, and chemoresistance

We also analyzed in MDA-MB-231 USP27X KO cells other characteristics dependent on Snail1 expression. USP27X KO cells or cells transfected with a *USP27X* siRNA exhibited impaired cell migration or cell invasion through Matrigel or Collagen I–coated Transwells (Fig. 4A and B); this inhibition was similar to that observed with an *SNAI1* siRNA (Fig. 4A). Importantly, Snail1 overexpression rescued cell invasion in USP27X KO cells (Fig. 4B). The metastatic potential was also assessed after intravenous inoculation of 1×10^6 cells of WT, USP27X KO, and USP27X KO-Snail1 cells expressing luciferase into NOD/SCID mice. *In vivo* bioluminescent imaging showed that WT cells consistently originated lung metastasis after 21 days (when control mice were euthanized to avoid animal suffering); in contrast, USP27X KO cells showed only residual luciferase activity in the lung till the end of the experiment (day 40; Fig. 4C). Snail1 ectopic expression in USP27X KO cells partially rescued metastasis formation after 3 weeks, being luciferase activity highly increased after 5 weeks, although USP27X KO-Snail1 cells never reached the levels of WT (Fig. 4C and D). *Ex vivo* quantification of luminescence gave similar results (Fig. 4E). Postmortem histologic analysis of lungs revealed a high number of metastatic foci generated by WT cells and USP27X KO-Snail1 cells, which were absent for USP27X KO cells (Fig. 4F). These results clearly showed that USP27X was critical for extravasation and/or colonization of the lung by breast tumor cells and that this effect was significantly dependent on Snail1 expression.

Snail1 is upregulated by chemotherapeutic agents and increases resistance to cell death triggered by these compounds (30). Western blot analysis showed a clear increase of Snail1 in WT cells upon addition of cisplatin (Fig. 5A), consistent with an *SNAI1* mRNA upregulation (Fig. 5B). USP27X remained constant. In contrast, Snail1 protein was not upregulated by cisplatin in USP27X KO cells (Fig. 5A), despite *SNAI1* mRNA was raised similarly to WT cells (Fig. 5B). These results suggest that Snail1 stabilization after treatment with this drug requires the participation of USP27X. We also determined the effect of USP27X

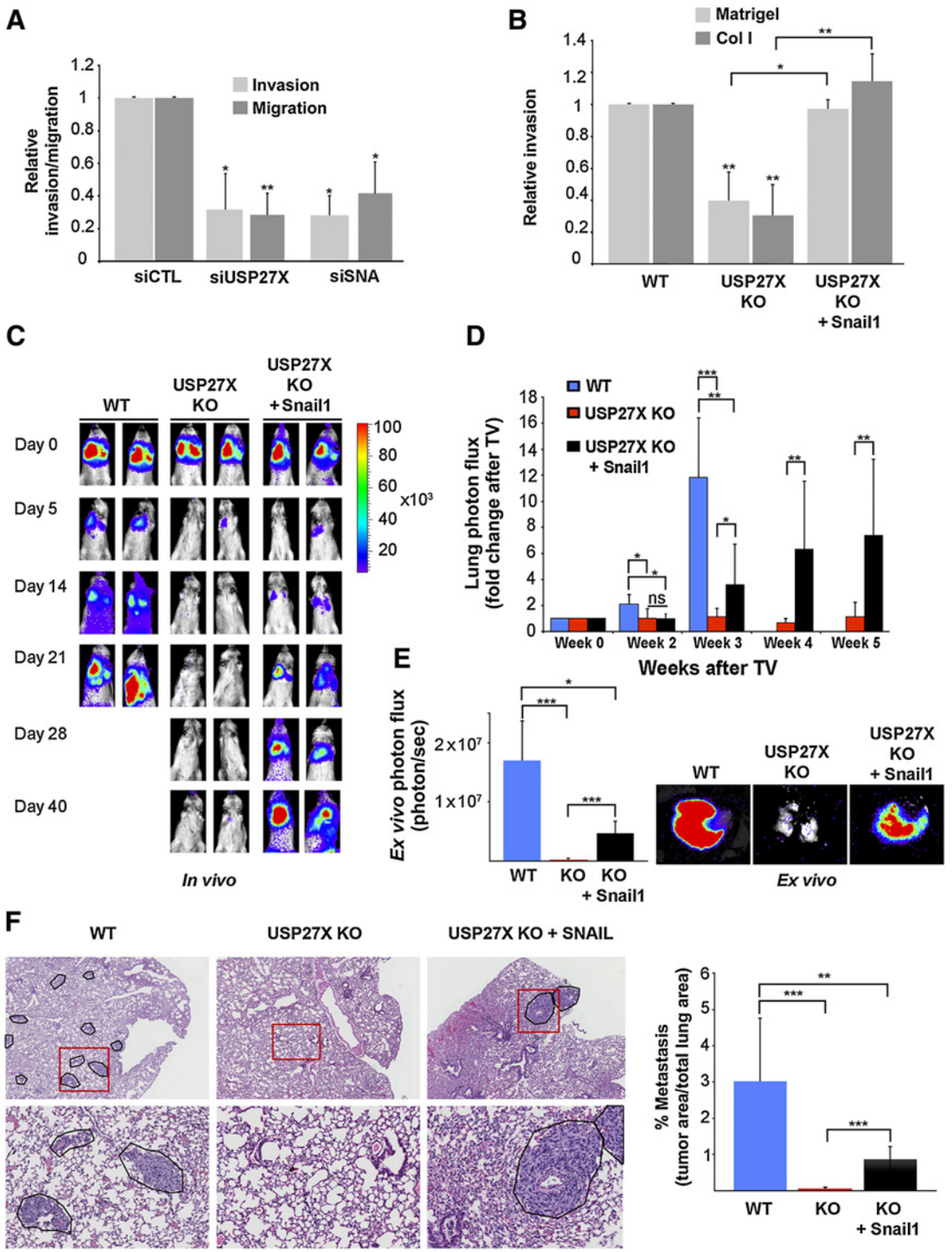

Figure 4.

USP27X depletion decreases cell migration, invasion, and metastasis. **A,** MDA-MB-231 cells were transfected with the indicated siRNAs, plated on Matrigel-coated Transwells (50,000 cells/well), and invasion toward 10% FBS was assessed after 10 hours. Cell migration was performed without Matrigel for 6 hours. **B,** MDA-MB-231 WT, USP27X KO, and USP27X KO + Snail1 cells were seeded on Matrigel or Collagen I–coated Transwells as in **A**. Invasion and migration assays were quantified with ImageJ after fixation and staining with DAPI; the figure shows the mean ± SD of three independent experiments. **C,** *In vivo* bioluminescence detection at indicated times of lung metastasis in NOD/SCID mice after tail-vein (TV) injection of MDA-MB-231 WT, USP27X KO, and USP27X KO + Snail1 cells, all expressing luciferase. IVIS images are representative of two mice from eight. Color bar is shown for photon flux equivalence. **D,** Quantification of bioluminescence at indicated times ($n = 8$). Data are the normalized photon flux represented as a fold change after tail-vein injection. **E,** *Ex vivo* bioluminescence quantification of lungs determined immediately after mice were euthanized (WT, day 21; USP27X KO and USP27X KO + Snail1, day 40). Right, representative IVIS images of metastatic lungs *ex vivo*. **F,** Left, H&E staining of histologic lung sections after the completion of the experiment described above (WT, day 21; USP27X KO and USP27X KO + Snail1, day 40). Top, metastases are marked with lines (×10); bottom, magnification of metastatic areas indicated with red squares (×20). Right, metastatic area quantification per total lung after scoring 10 representative sections. Data are the mean ± SD; *, $P < 0.05$; **, $P < 0.01$; ***, $P < 0.001$.

expression on the viability of MDA-MB-231 cells in the presence of cisplatin. Exposure to the drug was limited to 48 hours, a time where the differences in cell growth between WT and USP27X KO cells were not significant yet (see Fig. 3B). USP27X depletion strongly affected cisplatin sensitivity because KO cells showed a much lower IC_{50} (9 μmol/L) than WT cells (30 μmol/L; Fig. 5C). Importantly, Snail1 reexpression in USP27X KO cells rescued cell survival to a similar extent than that observed in WT cells (Fig. 5C). According with this, the quantification of apoptotic cells (early and late apoptosis) after cisplatin treatment showed a higher number in USP27X KO cells than in WT cells (Fig. 5D). Snail1 reexpression in USP27X KO cells significantly decreased the number of apoptotic cells after cisplatin addition (Fig. 5D). Overall, these results show that USP27X depletion enhances sensitivity to cisplatin and apoptosis in a Snail1-dependent fashion.

USP27X is critical for TGFβ-dependent EMT and fibroblast activation

The cytokine TGFβ induces an EMT (1) in the normal murine mammary NMuMG cells initiated by the rapid increase in Snail1 expression (31, 32). Interestingly, the expression of USP27X was also strongly upregulated by TGFβ both at mRNA and protein levels (Fig. 6A and B). Snail1 protein levels were not stimulated by TGFβ in USP27X KO cells (Fig. 6A). Accordingly, the Snail1 downstream target fibronectin was upregulated at 24 hours of treatment in WT but not in USP27X KO cells (Fig. 6A). The inability of TGFβ to promote an EMT in USP27X KO cells was not due to a general inhibition of TGFβ signaling because phospho-Smad2 was increased in both WT and KO cells (Fig. 6A). In accordance with the induction of Snail1 and fibronectin by TGFβ, this cytokine significantly boosted migration and invasion through Collagen I (4-fold and 6-fold, respectively, in TGFβ treated vs. control cells); this stimulation was completely abrogated in USP27X KO cells (Fig. 6C). The absence of USP27X also affected other genes modulated by TGFβ downstream of Snail1: *Cdh1* RNA was much more rapidly repressed in WT cells upon TGFβ treatment than in USP27X KO cells, whereas the mesenchymal marker *Zeb1* showed a much higher rise in WT cells than in USP27X KO cells (Fig. 6D). *Snai1* mRNA increased in a time-dependent fashion in both WT and KO cells (Fig. 6D), reinforcing the idea that KO cells respond to TGFβ similar to WT cells. In fact, the upregulation of *Snai1* mRNA by TGFβ was even higher in USP27X KO than in WT cells, suggesting the existence of a Snail1 self-regulatory inhibition (33). Confocal immunofluorescence analysis also showed that USP27X, Snail1, and fibronectin were

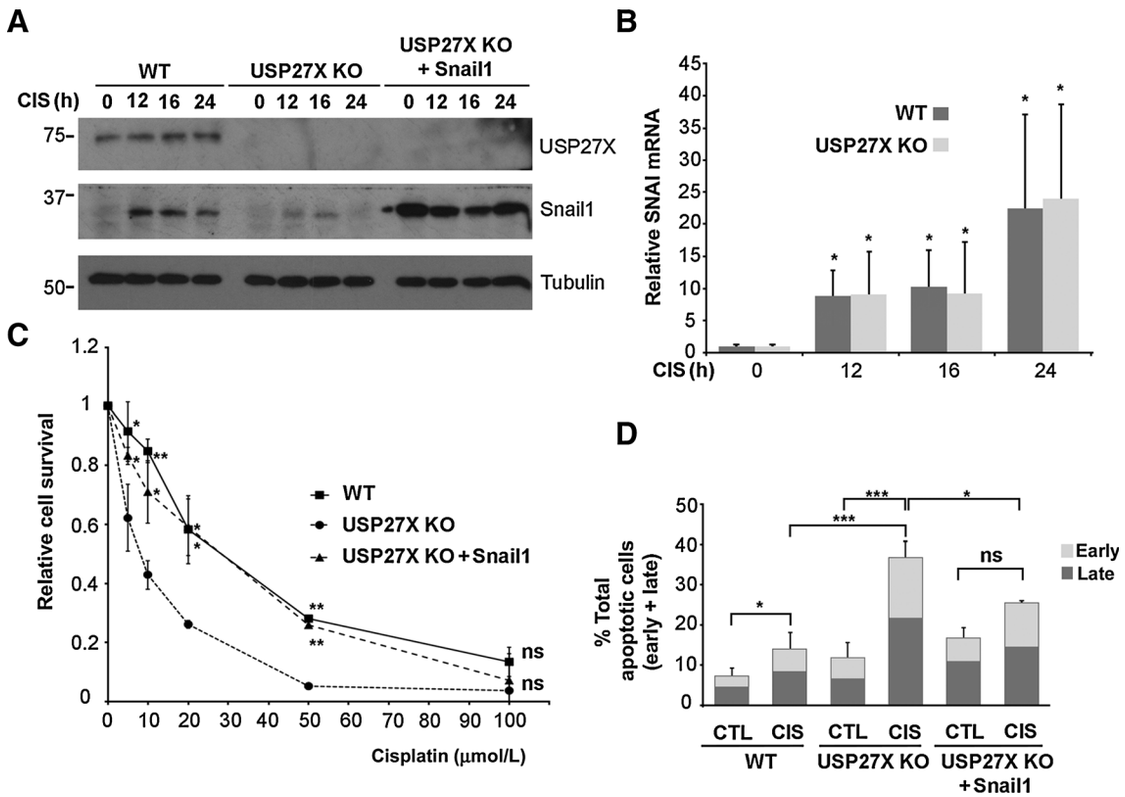

Figure 5.

USP27X depletion enhances cisplatin toxicity. **A** and **B,** Western blot analysis of Snail1 and USP27X (**A**) and *SNAI1* mRNA quantification (**B**) after treatment with 40 μmol/L cisplatin (CIS) of MDA-MB-231 WT, USP27X KO, and USP27X KO + Snail1 cells. **C,** Quantification of cell survival by MTT after 48 hours of treatment with increasing concentrations of CIS. Data were normalized to time 0 and to the corresponding untreated cells. The figure represents the mean ± SD of three independent experiments. **D,** Quantification of total (early and late) apoptosis by FACS analysis after Annexin V and 7-amino-actinomycin D (7-AAD) staining of cells treated with CIS for 24 hours. The individual values of Annexin V^+ (early apoptotic) cells and Annexin V^+/7-AAD^+ (late apoptotic) cells are indicated. Data, mean ± SD ($n = 4$). *, $P < 0.05$; **, $P < 0.01$; ***, $P < 0.001$; ns, not significant. *P* values in **C** refer to WT and USP27X KO + Snail1 cells compared with USP27X KO cells.

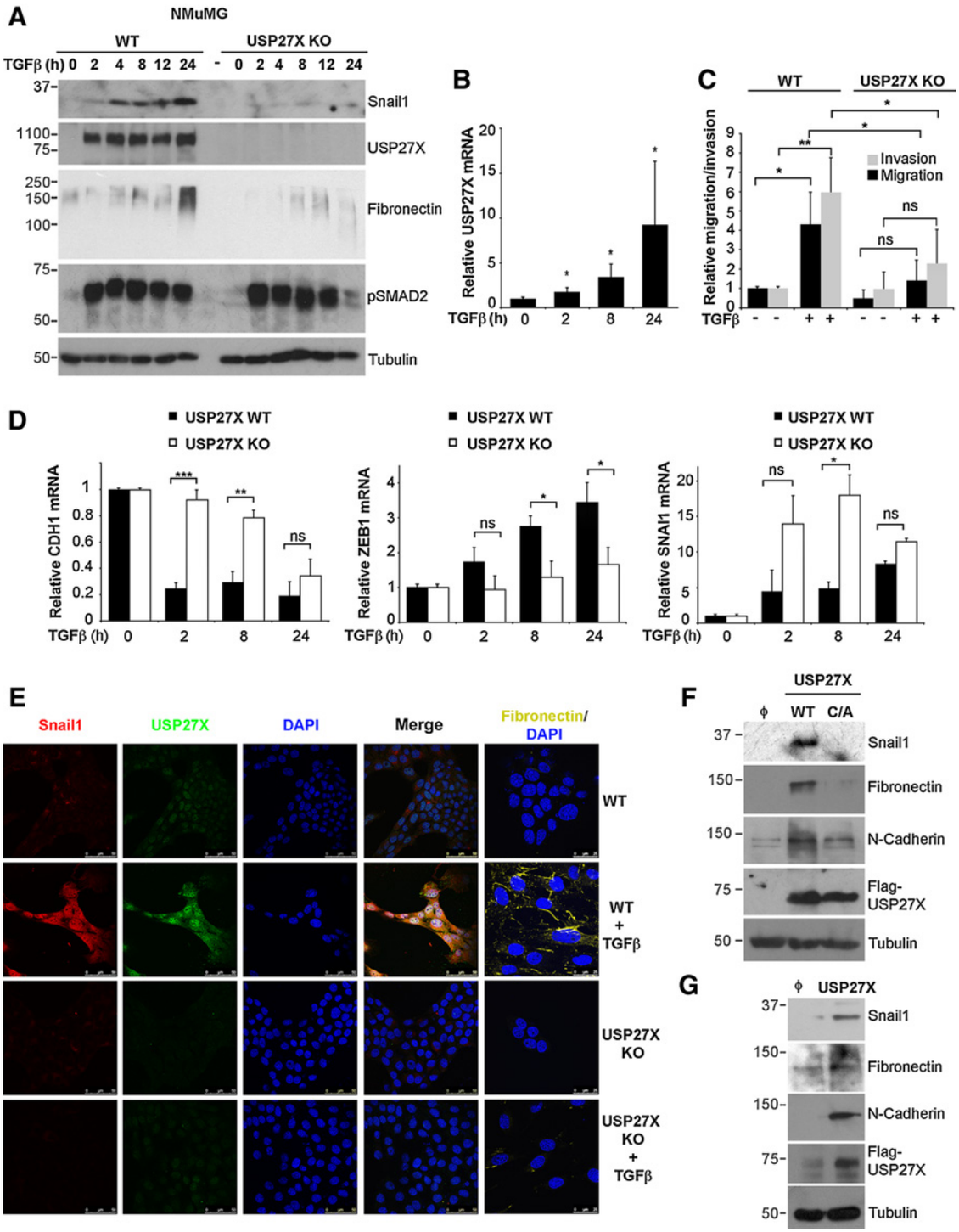

Figure 6.

TGFβ upregulates USP27X to stabilize Snail1 during EMT. **A,** NMuMG cells (WT or USP27X KO) were treated with 5 ng/mL TGFβ for the indicated times and analyzed by Western blotting. pSMAD2 was used as a positive control of TGFβ stimulation. **B,** *USP27X* mRNA quantification by qRT-PCR after treatment with TGFβ of NMuMG cells. Data represent the media ± SD of three independent experiments. **C,** NMuMG control (WT) or USP27X KO cells were treated during 24 hours with TGFβ, and migration and invasion through Collagen I was evaluated after 8 or 16 hours, respectively. The graph shows the quantification (mean ± SD; $n = 3$). **D,** mRNA from the indicated genes was assessed by qRT-PCR in USP27X WT and USP27X KO cells (mean ± SD; $n = 3$). **E,** Immunofluorescence analysis of endogenous Snail1 and USP27X (×40) or fibronectin (×60) from NMuMG WT and USP27X KO cells treated with TGFβ for 24 hours. DAPI staining was used for visualizing the nuclei. **F** and **G,** Transfection of the 50-KDa WT and C/A mutant (**F**), or the 72-KDa USP27X (**G**) and analysis of proteins upregulated in EMT (Snail1, fibronectin, and N-cadherin). *, $P < 0.05$; **, $P < 0.01$; ***, $P < 0.001$.

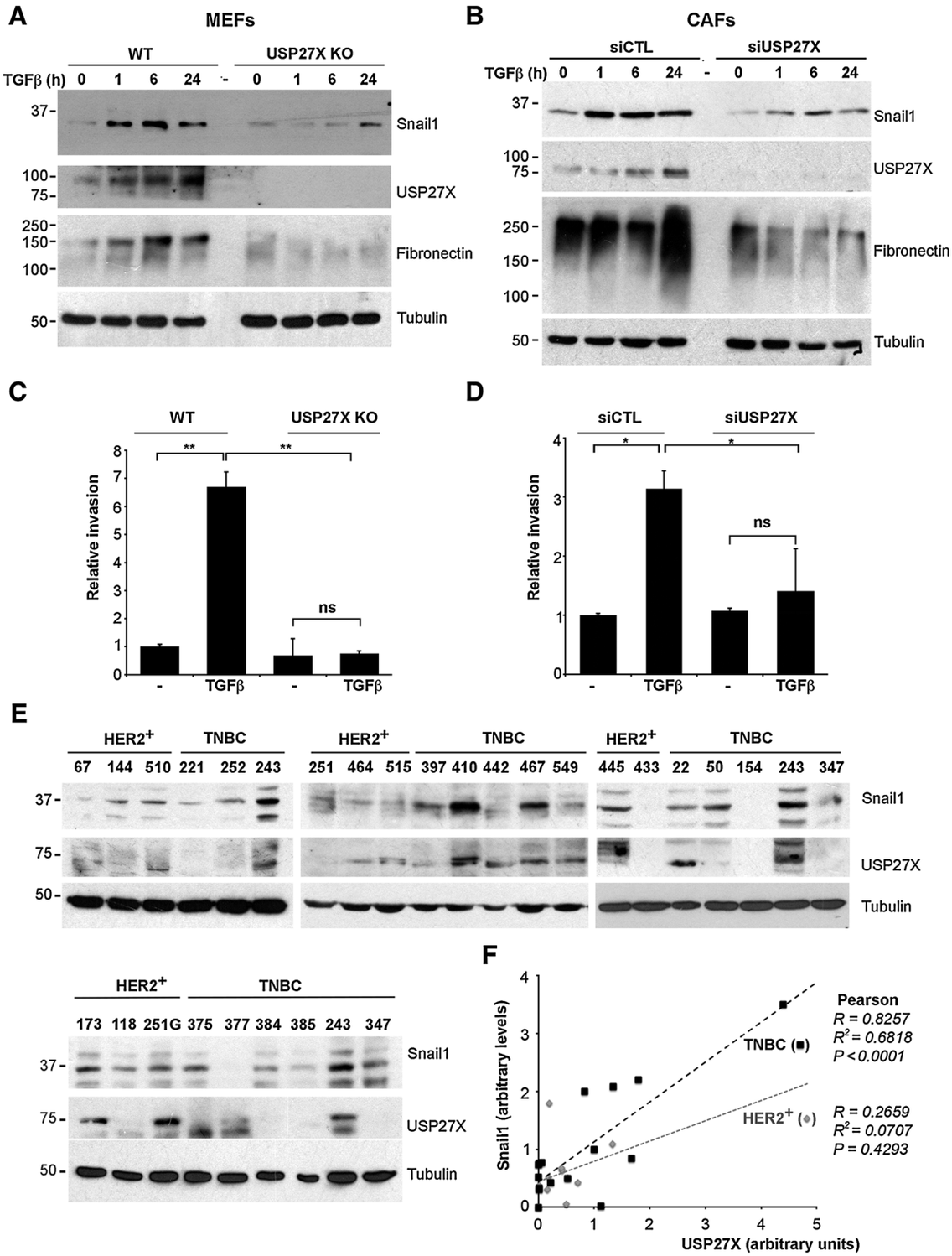

Figure 7.

Expression of Snail1 depends on USP27X in activated fibroblasts and tumor cancer cells. **A** and **B,** Analysis of Snail1 in WT or USP27X KO MEFs cells (**A**) and in mCAFs transfected with siCTL or si*USP27X* (**B**). Cells were treated with 5 ng/mL TGFβ for the indicated times. **C** and **D,** MEFs (WT or USP27X KO; **C**) or mCAFs (**D**) were treated with TGFβ during 24 hours to assess cell invasion during 16 hours on Matrigel (**C**) or Collagen I (**D**)–coated Transwells. The graph shows the mean ± SD of three independent experiments. *, $P < 0.05$; **, $P < 0.01$; ns, not significant. **E,** Snail1 and USP27X expression was determined in protein extracts from breast cancer PDXs classified as HER2$^+$ or triple negative (TNBC). The high-expressing Snail1 and USP27X tumor number PDX 243 was included in several blots as an internal control. **F,** Snail1 and USP27X expression was analyzed by densitometry with ImageJ in 27 PDX tumors and is represented as a scatter plot. The Pearson correlation coefficient was individually calculated for the HER2$^+$ and TNBC groups. Statistical significance was determined by two-tailed, unpaired *t* test, and specific *P* values are indicated.

upregulated by TGFβ in control but not in USP27X KO cells (Fig. 6E). Both USP27X and Snail1 were preferentially nuclear in TGFβ-treated cells, although they also showed a partial cytoplasmic localization (Fig. 6E). Finally, ectopic expression of USP27X, either the 50 kDa or 72 kDa forms in NMuMG cells recapitulated the EMT program triggered by TGFβ because it increased Snail1, fibronectin, and N-cadherin expression (Fig. 6F and G).

The TGFβ/Snail1 axis is also required for fibroblast activation (20). Similarly to that observed in epithelial cells, TGFβ also increases USP27X and Snail1 in control MEFs and in mCAFs obtained from PyMT-MMTV breast tumors (Figs. 7A and B) but not in MEFs KO for USP27X or mCAFs after silencing of USP72X by siRNA. In both cell systems, USP27X depletion also affected the upregulation of fibronectin (Fig. 7A and B) and cell invasion (Fig. 7C and D) by TGFβ. Altogether, these results indicate that Snail1 protein stabilization by USP27X is a key event to develop a full EMT and fibroblast activation in response to TGFβ.

USP27X and Snail1 protein expression correlates in tumors

A transcriptomic analysis of USP27X in a public database showed a significant increase in patients with breast, pancreatic, and colorectal cancer (Supplementary Fig. S8). Because of the high expression of USP27X in breast cancer cell lines, we also analyzed the expression in a panel of 27 patient-derived xenografted (PDX) human breast tumors corresponding to $HER2^+$ and triple-negative breast neoplasms (TNBC). PDXs recapitulate and preserve most of the traits from the patient sample at the transcriptomic, epigenomic, and histologic levels (34). Western blot (Fig. 7E) and densitometric analysis (Fig. 7F) showed a significant correlation between Snail1 and USP27X in TNBC but not in $HER2^+$ tumors. These results reinforce the hypothesis that Snail1 requires USP27X to be efficiently expressed in TNBC cells.

Discussion

In this article, we have identified USP27X as a highly active Snail1 DUB using an siRNA functional screening. This approach has been shown to be a valuable tool to characterize new kinases and ubiquitin ligases controlling Snail1 protein stability (12, 23, 35). Besides USP27X, three other DUBs were identified in our screening—MPND, VCPIP1, and OTUD7A/CEZANNE2—that stabilized Snail1, although they did not associate with this factor in coimmunoprecipitation experiments. However, MPND and Cezanne2 slightly interact with Snail1 after proteasome inhibition (Supplementary Fig. S2C), suggesting that accumulation of polyubiquitinated Snail1 might favor the association with these particular DUBs. They might also regulate Snail1 indirectly, as indicated above or even controlling the stability of USP27X. Curiously, our screening also detected other DUBs depletion of which enhances Snail1-F-Luc/R-Luc (Fig. 1A). Probably, these DUBs might remove other ubiquitination events that have been associated with Snail1 stability, such as Snail1 K63 polyubiquitination mediated by Pellino E3 ligase (36) or A20-dependent Snail1 multimonoubiquitination (37).

Snai1l ubiquitination occurs in the cytoplasm by the highly active ubiquitin ligases β-TrCP1 (Fbxw1) and Fbxl14, or in the nucleus, by Fbxl5 or Fbxo11 (9). Wherever Snail1 ubiquitination takes place, inhibition of nuclear export stabilizes Snail1, suggesting that degradation happens in the cytosol (9). USP27X contains a nuclear localization signal (22) and target nuclear substrates such as histone H2B or the transcription factor Hes1 (22, 27). Accordingly, USP27X might act on both nuclear and cytosolic Snail1; however, our data suggest that Snail1 deubiquitination likely occurs in the cytoplasm. This hypothesis is supported by experiments showing a strong stabilization of Snail1-SD mutant that is mostly localized in the cytosol and by immunofluorescence analyses showing USP27X presence in both the nucleus and cytosol. USP27X action in the cytosol has also been demonstrated by other authors (24). However, we cannot discard the possibility that nuclear deubiquitination also contributes to Snail1 stability by blocking nuclear export and favoring Snail1 nuclear retention. Regardless of whether Snail1 deubiquitination happens in the nucleus or cytosol, in both cases it contributes to Snail1 stability.

The USP27X homologous protein USP22 also interacts and stabilizes Snail1 (see Supplementary Fig. S4). However, inhibition of USP22 was not found to significantly decrease Snail1-F-Luc/R-Luc in the screening. Moreover, its endogenous levels cannot compensate the lack of USP27X in KO cells in the different cell lines analyzed. This suggests that USP27X has a predominant role in Snail1 deubiquitination *in vivo*, although we cannot discard that USP22 may substitute USP27X and participate in Snail1 stabilization in other cells or upon other stimuli, because many pieces of evidence support the functional relationship between USP22 and USP27X on other substrates. USP22 was first identified as an H2B deubiquitinase being part of the SAGA complex (38, 39). Depletion of USP22 favors USP27X (and also USP51) deubiquitination of H2B independently of SAGA (22). USP27X or USP22 depletion enhances sensitivity to cisplatin (Fig. 5) or to 5-fluoruacil (40), respectively, suggesting a functional relationship. Moreover, USP22 is associated with EMT in colorectal (41), lung (42), and pancreatic tumors (43). This action of USP22 might be related to its activity on nonhistone substrates such as c-Myc and Hes1 (27, 44, 45). Further work is needed to clarify the putative role of USP22 as a possible Snail1 DUB.

We have observed a significant correlation between Snail1 and USP27X in PDX derived from TNBC tumors by Western blot. Unfortunately, no studies have so far analyzed the expression of USP27X in tumors due to the absence of good antibodies to detect this protein in paraffin-embedded samples. Specific studies directed to analyze USP27X in tumor samples are required to verify its relative contribution during cancer progression.

While this study was being performed, two groups reported that Snail1 is deubiquitinated by DUB3 (also known as USP17L2; refs. 17, 18). In our screening, DUB3 inhibition decreased Snail1-F-Luc/R-Luc by 2-fold, less than the threshold preestablished in our screening, and therefore this DUB was not initially selected. Anyway, we compared DUB3 and USP27X effects on Snail1: both DUBs stabilize and interact with Snail1, although USP27X seems to be more potent (Supplementary Fig. S6E–S6G). Moreover, USP27X and DUB3 present several differences. DUB3 is associated with the Snail1 N-terminal domain (18), whereas USP27X requires the C-terminal fragment. DUB3 also binds and stabilizes Snail2 (Slug) and Twist (46), whereas the action of USP27X on Snail2 is likely indirect because both proteins do not physically interact. Curiously, both DUB3 and USP27X proteases are also stimulated by cytokines; whereas USP27X is rapidly and potently stimulated by TGFβ, DUB3 is induced by IL6 (18), a cytokine also linked to

EMT (47). It remains to be established whether Snail1 induction caused by IL6 or other cytokines in other cells require the expression of USP27X, DUB3, or a different DUB.

Snail1 transcriptional factor plays a key relevant action in several cellular traits related to tumor growth and progression because it promotes tumor invasion, resistance to classic antineoplastic agents, acquisition of cancer stem cell characteristics, and activation of cancer-activated fibroblasts (3, 20, 48). Therefore, Snail1 is an attractive target for chemotherapy. However, inhibitors of Snail1 function have not been characterized so far, a fact probably related to the lack of enzymatic activity of this protein. Snail1 is a very unstable protein, and its half-life is dependent on the coordinated action of several ubiquitin ligases and DUBs. Because developing E3s agonists is extremely challenging, an alternative and much more feasible possibility consists in generating DUB inhibitors that affect Snail1 expression and function. The characterization of USP27X as a very active Snail1 DUB provides new opportunities for the development of new molecules that specifically interfere with Snail1 expression and opens new lines for the treatment of cancer metastasis.

Disclosure of Potential Conflicts of Interest

J. Arribas reports receiving other commercial research support from Hofman La Roche, Synthon, and Molecular Partners and is a consultant/advisory board member for Menarini Biotech. No potential conflicts of interest were disclosed by the other authors.

Authors' Contributions

Conception and design: A. García de Herreros, V.M. Díaz
Development of methodology: G. Lambies, C. Martínez-Guillamon, R. Olivera-Salguero, R. Peña, V.M. Díaz
Acquisition of data (provided animals, acquired and managed patients, provided facilities, etc.): G. Lambies, M. Miceli, C. Martínez-Guillamon, C.-P. Frías, I. Calderón, S.Y.R. Dent, J. Arribas
Analysis and interpretation of data (e.g., statistical analysis, biostatistics, computational analysis): G. Lambies, M. Miceli, C. Martínez-Guillamon, R. Olivera-Salguero, R. Peña, A. García de Herreros, V.M. Díaz
Writing, review, and/or revision of the manuscript: G. Lambies, S.Y.R. Dent, J. Arribas, A. García de Herreros, V.M. Díaz
Administrative, technical, or material support (i.e., reporting or organizing data, constructing databases): R. Peña, C.-P. Frías, I. Calderón
Study supervision: V.M. Díaz
Other (provided critical reagents including USP27X specific antibodies and expression vectors; discussed the results in the manuscript): B.S. Atanassov

Acknowledgments

We thank Drs. Yibin Kang (Princeton University, Princeton, New Jersey), Arnim Weber and Georg Häcker (University Medical Center Freiburg, Germany), Taeko Kobayashi (Institute for Virus Research, Kyoto University), Yadi Wu (The University of Kentucky, Lexington, Kentucky), and Cristina Fillat (IDIBAPS, Barcelona, Spain) for kindly sending plasmids and for advice. We really appreciate the technical support of Jordi Vergés and Cristina Bernardo. This study was funded by grants awarded by Ministerio de Economía y Competitividad (MINECO) and Fondo Europeo de Desarrollo Regional-FEDER to A. García de Herreros (SAF2013-48849-C2-1-R and SAF2016-76461-R) and to V.M. Díaz (SAF2013-48849-C2-2-R). Research at the A. García de Herreros lab is supported by funds from the Fundación Científica de la Asociación Española contra el Cáncer and from the Instituto de Salud Carlos III (PIE15/00008). Research at the B.S. Atanassov lab is supported by the Rosswell Park Cancer Institute and NCI grant P30CA016056. Research at the J. Arribas lab is supported by funds from the Breast Cancer Research Foundation (BCRF-17-008) and Instituto de Salud Carlos III (PI16/00253).

The costs of publication of this article were defrayed in part by the payment of page charges. This article must therefore be hereby marked *advertisement* in accordance with 18 U.S.C. Section 1734 solely to indicate this fact.

Received March 10, 2018; revised September 14, 2018; accepted October 15, 2018; published first October 19, 2018.

References

1. Nieto MA, Huang RY, Jackson RA, Thiery JP. Emt: 2016. Cell 2016;166:21–45.
2. Thiery JP, Acloque H, Huang RY, Nieto MA. Epithelial–mesenchymal transitions in development and disease. Cell 2009;139:871–90.
3. Baulida J, Garcia de Herreros A. Snail1-driven plasticity of epithelial and mesenchymal cells sustains cancer malignancy. Biochim Biophys Acta 2015;1856:55–61.
4. Shibue T, Weinberg RA. EMT, CSCs, and drug resistance: the mechanistic link and clinical implications. Nat Rev Clin Oncol 2017;14:611–29.
5. Rhim AD, Mirek ET, Aiello NM, Maitra A, Bailey JM, McAllister F, et al. EMT and dissemination precede pancreatic tumor formation. Cell 2012;148:349–61.
6. Imani S, Hosseinifard H, Cheng J, Wei C, Fu J. Prognostic Value of EMT-inducing transcription factors (EMT-TFs) in metastatic breast cancer: a systematic review and meta-analysis. Sci Rep 2016;6:28587.
7. Weissman AM, Shabek N, Ciechanover A. The predator becomes the prey: regulating the ubiquitin system by ubiquitylation and degradation. Nat Rev Mol Cell Biol 2011;12:605–20.
8. Diaz VM, Viñas-Castells R, Garcia de Herreros A. Regulation of the protein stability of EMT transcription factors. Cell Adh Migr 2014;8:418–28.
9. Diaz VM, García de Herreros A. F-box proteins: Keeping the epithelial-to-mesenchymal transition (EMT) in check. Semin Cancer Biol 2016;36:71–9.
10. Escriva M, Peiro S, Herranz N, Villagrasa P, Dave N, Montserrat-Sentis B, et al. Repression of PTEN phosphatase by Snail1 transcriptional factor during gamma radiation-induced apoptosis. Mol Cell Biol 2008;28:1528–40.
11. Kurrey NK, Jalgaonkar SP, Joglekar AV, Ghanate AD, Chaskar PD, Doiphode RY, et al. Snail and slug mediate radioresistance and chemoresistance by antagonizing p53-mediated apoptosis and acquiring a stem-like phenotype in ovarian cancer cells. Stem Cells 2009;27:2059–68.
12. Viñas-Castells R, Frias A, Robles-Lanuza E, Zhang K, Longmore GD, Garcia de Herreros A, et al. Nuclear ubiquitination by FBXL5 modulates Snail1 DNA binding and stability. Nucleic Acids Res 2014;42:1079–94.
13. Viñas-Castells R, Beltran M, Valls G, Gomez I, Garcia JM, Montserrat-Sentis B, et al. The hypoxia-controlled FBXL14 ubiquitin ligase targets SNAIL1 for proteasome degradation. J Biol Chem 2010;285:3794–805.
14. Frias A, Lambies G, Viñas-Castells R, Martinez-Guillamon C, Dave N, Garcia de Herreros A, et al. A Switch in Akt isoforms is required for notch-induced snail1 expression and protection from cell death. Mol Cell Biol 2015;36:923–40.
15. Komander D, Clague MJ, Urbe S. Breaking the chains: structure and function of the deubiquitinases. Nat Rev Mol Cell Biol 2009;10:550–63.
16. Wei R, Liu X, Yu W, Yang T, Cai W, Liu J, et al. Deubiquitinases in cancer. Oncotarget 2015;6:12872–89.
17. Liu T, Yu J, Deng M, Yin Y, Zhang H, Luo K, et al. CDK4/6-dependent activation of DUB3 regulates cancer metastasis through SNAIL1. Nat Commun 2017;8:13923.
18. Wu Y, Wang Y, Lin Y, Liu Y, Wang Y, Jia J, et al. Dub3 inhibition suppresses breast cancer invasion and metastasis by promoting Snail1 degradation. Nat Commun 2017;8:14228.
19. Young L, Sung J, Stacey G, Masters JR. Detection of Mycoplasma in cell cultures. Nat Protoc 2010;5:929–34.
20. Alba-Castellon L, Olivera-Salguero R, Mestre-Farrera A, Pena R, Herrera M, Bonilla F, et al. Snail1-dependent activation of cancer-associated fibroblast

controls epithelial tumor cell invasion and metastasis. Cancer Res 2016; 76:6205–17.
21. Franci C, Takkunen M, Dave N, Alameda F, Gomez S, Rodriguez R, et al. Expression of Snail protein in tumor-stroma interface. Oncogene 2006;25: 5134–44.
22. Atanassov BS, Mohan RD, Lan X, Kuang X, Lu Y, Lin K, et al. ATXN7L3 and ENY2 coordinate activity of multiple H2B deubiquitinases important for cellular proliferation and tumor growth. Mol Cell 2016;62:558–71.
23. Zheng H, Shen M, Zha YL, Li W, Wei Y, Blanco MA, et al. PKD1 phosphorylation-dependent degradation of SNAIL by SCF-FBXO11 regulates epithelial-mesenchymal transition and metastasis. Cancer Cell 2014;26: 358–73.
24. Weber A, Heinlein M, Dengjel J, Alber C, Singh PK, Hacker G. The deubiquitinase Usp27x stabilizes the BH3-only protein Bim and enhances apoptosis. EMBO Rep 2016;17:724–38.
25. Altun M, Kramer HB, Willems LI, McDermott JL, Leach CA, Goldenberg SJ, et al. Activity-based chemical proteomics accelerates inhibitor development for deubiquitylating enzymes. Chem Biol 2011;18:1401–12.
26. Knab LM, Ebine K, Chow CR, Raza SS, Sahai V, Patel AP, et al. Snail cooperates with Kras G12D in vivo to increase stem cell factor and enhance mast cell infiltration. Mol Cancer Res 2014;12:1440–8.
27. Kobayashi T, Iwamoto Y, Takashima K, Isomura A, Kosodo Y, Kawakami K, et al. Deubiquitinating enzymes regulate Hes1 stability and neuronal differentiation. FEBS J 2015;282:2411–23.
28. Clague MJ, Barsukov I, Coulson JM, Liu H, Rigden DJ, Urbe S. Deubiquitylases from genes to organism. Physiol Rev 2013;93:1289–315.
29. Dominguez D, Montserrat-Sentis B, Virgos-Soler A, Guaita S, Grueso J, Porta M, et al. Phosphorylation regulates the subcellular location and activity of the snail transcriptional repressor. Mol Cell Biol 2003;23: 5078–89.
30. Hsu DS, Lan HY, Huang CH, Tai SK, Chang SY, Tsai TL, et al. Regulation of excision repair cross-complementation group 1 by Snail contributes to cisplatin resistance in head and neck cancer. Clin Cancer Res 2010;16: 4561–71.
31. Dave N, Guaita-Esteruelas S, Gutarra S, Frias A, Beltran M, Peiro S, et al. Functional cooperation between Snail1 and twist in the regulation of ZEB1 expression during epithelial to mesenchymal transition. J Biol Chem 2011;286:12024–32.
32. Deckers M, van Dinther M, Buijs J, Que I, Lowik C, van der Pluijm G, et al. The tumor suppressor Smad4 is required for transforming growth factor beta-induced epithelial to mesenchymal transition and bone metastasis of breast cancer cells. Cancer Res 2006;66:2202–9.
33. Peiro S, Escriva M, Puig I, Barbera MJ, Dave N, Herranz N, et al. Snail1 transcriptional repressor binds to its own promoter and controls its expression. Nucleic Acids Res 2006;34:2077–84.
34. Byrne AT, Alferez DG, Amant F, Annibali D, Arribas J, Biankin AV, et al. Interrogating open issues in cancer precision medicine with patient-derived xenografts. Nat Rev Cancer 2017;17:254–68.
35. Zhang K, Rodriguez-Aznar E, Yabuta N, Owen RJ, Mingot JM, Nojima H, et al. Lats2 kinase potentiates Snail1 activity by promoting nuclear retention upon phosphorylation. Embo J 2012;31:29–43.
36. Jeon YK, Kim CK, Hwang KR, Park HY, Koh J, Chung DH, et al. Pellino-1 promotes lung carcinogenesis via the stabilization of Slug and Snail through K63-mediated polyubiquitination. Cell Death Differ 2017;24: 469–80.
37. Lee JH, Jung SM, Yang KM, Bae E, Ahn SG, Park JS, et al. A20 promotes metastasis of aggressive basal-like breast cancers through multi-monoubiquitylation of Snail1. Nat Cell Biol 2017;19:1260–73.
38. Zhang XY, Varthi M, Sykes SM, Phillips C, Warzecha C, Zhu W, et al. The putative cancer stem cell marker USP22 is a subunit of the human SAGA complex required for activated transcription and cell-cycle progression. Mol Cell 2008;29:102–11.
39. Zhao Y, Lang G, Ito S, Bonnet J, Metzger E, Sawatsubashi S, et al. A TFTC/STAGA module mediates histone H2A and H2B deubiquitination, coactivates nuclear receptors, and counteracts heterochromatin silencing. Mol Cell 2008;29:92–101.
40. Zhang J, Luo N, Tian Y, Li J, Yang X, Yin H, et al. USP22 knockdown enhanced chemosensitivity of hepatocellular carcinoma cells to 5-Fu by up-regulation of Smad4 and suppression of Akt. Oncotarget 2017;8: 24728–40.
41. Li Y, Yang Y, Li J, Liu H, Chen F, Li B, et al. USP22 drives colorectal cancer invasion and metastasis via epithelial–mesenchymal transition by activating AP4. Oncotarget 2017;8:32683–95.
42. Hu J, Yang D, Zhang H, Liu W, Zhao Y, Lu H, et al. USP22 promotes tumor progression and induces epithelial–mesenchymal transition in lung adenocarcinoma. Lung Cancer 2015;88:239–45.
43. Ning Z, Wang A, Liang J, Xie Y, Liu J, Yan Q, et al. USP22 promotes epithelial-mesenchymal transition via the FAK pathway in pancreatic cancer cells. Oncol Rep 2014;32:1451–8.
44. Melo-Cardenas J, Zhang Y, Zhang DD, Fang D. Ubiquitin-specific peptidase 22 functions and its involvement in disease. Oncotarget 2016;7:44848–56.
45. Kim D, Hong A, Park HI, Shin WH, Yoo L, Jeon SJ, et al. Deubiquitinating enzyme USP22 positively regulates c-Myc stability and tumorigenic activity in mammalian and breast cancer cells. J Cell Physiol 2017; 232:3664–76.
46. Lin Y, Wang Y, Shi Q, Yu Q, Liu C, Feng J, et al. Stabilization of the transcription factors slug and twist by the deubiquitinase dub3 is a key requirement for tumor metastasis. Oncotarget 2017;8: 75127–40.
47. Wu Y, Deng J, Rychahou PG, Qiu S, Evers BM, Zhou BP. Stabilization of snail by NF-kappaB is required for inflammation-induced cell migration and invasion. Cancer Cell 2009;15:416–28.
48. Stanisavljevic J, Loubat-Casanovas J, Herrera M, Luque T, Pena R, Lluch A, et al. Snail1-expressing fibroblasts in the tumor microenvironment display mechanical properties that support metastasis. Cancer Res 2015;75:284–95.